Similarity solutions of a Becker–Döring system with time-dependent monomer input

2004 J. Phys. A: Math. Gen. 37 7823

(http://iopscience.iop.org/0305-4470/37/32/001)

INSTITUTE OF PHYSICS PUBLISHING JOURNAL OF PHYSICS A: MATHEMATICAL AND GENERAL

J. Phys. A: Math. Gen. **37** (2004) 7823–7841 PII: S0305-4470(04)80932-6

Similarity solutions of a Becker–Döring system with time-dependent monomer input

Jonathan A D Wattis

Theoretical Mechanics, School of Mathematical Sciences, University of Nottingham, University Park, Nottingham, NG7 2RD, UK

E-mail: Jonathan.Wattis@nottingham.ac.uk

Received 18 May 2004
Published 28 July 2004
Online at stacks.iop.org/JPhysA/37/7823
doi:10.1088/0305-4470/37/32/001

Abstract

We formulate the Becker–Döring equations for cluster growth in the presence of a time-dependent source of monomer input. In the case of size-independent aggregation and fragmentation rate coefficients we find similarity solutions which are approached in the large time limit. The form of the solutions depends on the rate of monomer input and whether fragmentation is present in the model; four distinct types of solution are found.

PACS numbers: 64.60.−i, 05.70.Fh, 82.60.Nh

1. Introduction

Until recently, self-similar behaviour in the Becker–Döring equations has been almost unknown. However self-similar behaviour in the Smoluchowski coagulation equations [24] is commonplace and widely studied, for example, see Leyvraz [17] for a recent review. In the pure aggregation formulation of the Smoluchowski model [24]

$$\frac{\mathrm{d}c_r}{\mathrm{d}t} = \frac{1}{2}\sum_{s=1}^{r-1} a_{s,r-s}c_s c_{r-s} - \sum_{s=1}^{\infty} a_{r,s}c_r c_s, \tag{1.1}$$

attraction to self-similar solutions is observed in the explicitly solveable cases $a_{r,s} = a$ and $a_{r,s} = ars$ as well as many other kernels. The former has the form $c_r(t) = t^{-2}\psi(r/t)$ with $\psi(\eta) = (4/a^2\varrho)\,\mathrm{e}^{-2a\eta/\varrho}$; existence and convergence results have been proved for various cases by Kreer [16], da Costa [7] and Menon and Pego [21, 22]. The gelling solution for the kernel $a_{r,s} = ars$ was first found by Leyvraz and Tschudi [18]. For arbitrary initial data, this system undergoes a gelation transition at $t_g = 1/a\sum_{r=1}^{\infty} r^2 c_r(0)$; for $t > t_g$ the solution has the form $c_r(t) = t^{-1}\phi_r$ with ϕ_r independent of time, which is formally a similarity solution, and attracting for all initial data.

Krapivsky and Redner [15] have studied the differences in asymptotic structure between constant monomer and constant mass formulations of aggregation problems. Their study, however, was on the Smoluchowski coagulation equations, which allow coalescence between clusters of any size, perturbed by the addition of either Becker–Döring aggregation or Becker–Döring fragmentation processes. The Smoluchowski coagulation equations in the presence of monomer input have been analysed by Davies *et al* [11] who highlighted the important role which self-similar behaviour plays in the kinetics of aggregation. Lushnikov and Kulmala [19, 20] have studied a continuous form of the Smoluchowski coagulation equations in the presence of an input term and analysed the existence and form of similarity solutions in the large-time limit.

In this paper we consider the Becker–Döring equations in the more general form

$$\dot{c}_1 = J_0(t) - J_1 - \sum_{r=1}^{\infty} J_r \tag{1.2}$$

$$\dot{c}_r = J_{r-1} - J_r \tag{1.3}$$

$$J_r = a_r c_1 c_r - b_{r+1} c_{r+1} \tag{1.4}$$

with $J_0(t)$ being a term representing the time-dependent input of monomers. This statement of the problem includes both of the more commonly quoted forms of the Becker–Döring equations. These are the constant monomer concentration formulation which corresponds to $J_0 = J_1 + \sum_{r=1}^{\infty} J_r$, giving $\dot{c}_1 = 0$; this form was originally studied by Becker and Doring in [3]; and the constant mass formulation, which corresponds to $J_0(t) \equiv 0$. This latter form was proposed by Penrose and Lebowitz [23] and conserves the total mass of the system, defined by

$$M_1(t) = \sum_{r=1}^{\infty} r c_r. \tag{1.5}$$

Explicit solution for the case of constant mass (that is $J_0 \equiv 0$) and pure aggregation ($b_r = 0$ for all r) with rates of the form $a_r = ar$ has been found by Brilliantov and Krapivsky [5]. The solution for the constant monomer formulation with $b_r = 0$ and $a_r = ar$ is given in King and Wattis [14]. Brilliantov and Krapivsky [5] also consider the case of constant input rate in the purely aggregative Becker–Döring system with aggregation rates given by $a_r = ar^{\gamma}$ and $0 \leqslant \gamma \leqslant 1$. The Becker–Döring system of equations with monomer input has also been studied by Blackman and Marshall [4], who consider a constant rate of input into a system with aggregation and fragmentation rates given by $a_r = ar^p$ and $b_r = br^{-q}$. Several authors have analysed systems similar to (1.2)–(1.4) in the context of epitaxial growth; for details, see the work of Bales and Chrzan [2], Evans and Bartlet [12] and Gibou *et al* [13]. We comment further on these works in the discussion.

We shall consider input rates of the more general form $J_0(t) = \alpha t^w$ and, as with the Smoluchowski equations, we find self-similar behaviour. However, we find self-similar solutions in the case *with* fragmentation as well as in the case of pure aggregation.

1.1. Time-dependent input

In this paper we will analyse the Becker–Döring system given by equations (1.2)–(1.4) with the addition of a source of monomer which increases the concentration at a rate given by $J_0(t) = \alpha t^w$ with $w > -1$. We consider the initial data $c_r(0) = 0$ for all r. The first moment

of the distribution, M_1, which is the total mass in the system (1.5), then satisfies $\dot{M}_1 = \alpha t^w$, thus

$$M_1 = \frac{\alpha t^{w+1}}{(w+1)} \tag{1.6}$$

provided $w > -1$. It is also useful to define the quantity M_0 given by

$$M_0 = \sum_{r=1}^{\infty} c_r, \tag{1.7}$$

which represents the total number of clusters (including monomers). In this paper we will restrict ourselves to aggregation and fragmentation rates which are independent of cluster size, that is we will assume $a_r = a$ and $b_r = b$ for all r. The restriction to size-independent rates enables us to develop explicit formulae for the large-time behaviour of all concentrations. We cover both the cases $b = 0$ and $b \neq 0$; however, the theory and results for these two cases are quite distinct so will be considered separately.

In the case of pure aggregation ($b = 0$) for $w = 0$ da Costa *et al* [8] have rigorously proved that

$$c_1 \to 0, \qquad M_0 \to +\infty, \qquad M_0 c_1 \to \alpha t^w \tag{1.8}$$

as well as $c_r \to 0$ as $t \to \infty$ for all r. We would like to know the parameter ranges of w for which such large-time asymptotic results hold, and if they persist, when fragmentation is reintroduced into the model (i.e. when $b \neq 0$).

2. The Becker–Döring system with fragmentation

2.1. Equilibrium theory

In the case of the constant mass Becker–Döring system there are equilibrium solutions, and the properties of these will be useful in deriving some of the following results. At equilibrium, all fluxes, $J_r = 0$, so that $c_r = (ac_1/b)^{r-1}c_1$, for arbitrary c_1. Such a solution has number and mass given by

$$M_0 = \frac{bc_1}{b - ac_1}, \qquad M_1 = \frac{b^2 c_1}{(b - ac_1)^2}. \tag{2.1}$$

The value of c_1 adopted by the system at equilibrium is determined by equating M_1 (2.1) with the initial mass of the system (1.5). For $c_1 < b/a$, both M_0 and M_1 are finite, they diverge as $c_1 \to b/a$, since in this limit $c_r = c_1$ for all r; and for $c_1 > b/a$ the distribution function c_r increases with size r. Thus if the mass or the number of clusters diverges, then the system cannot be converging to an equilibrium solution with $c_1 < b/a$, but rather must have $c_1 \to C \geqslant b/a$ or be attracted to some other non-equilibrium solution.

For $w < -1$, the problem with input must be reposed so that the input term in (1.2) is $J_0(t) = \alpha(t + t_0)^w$ rather than $J_0(t) = \alpha t^w$, since this latter form has a singularity at $t = 0$. With $t_0 > 0$, the total mass in the system is finite, being given by

$$M_1(t) = M_1(0) + \alpha\left(t_0^{w+1} - (t + t_0)^{w+1}\right)\big/(-1 - w). \tag{2.2}$$

We define ϱ_∞ to be the large time limit of $M_1(t)$, then the system as a whole will approach the solution $c_r = (a/b)^{r-1}c_1^r$ with c_1 given by

$$c_1 = \frac{b^2}{2a^2\varrho_\infty}\left(1 + \frac{2a\varrho_\infty}{b} - \sqrt{1 + \frac{4a\varrho_\infty}{b}}\right). \tag{2.3}$$

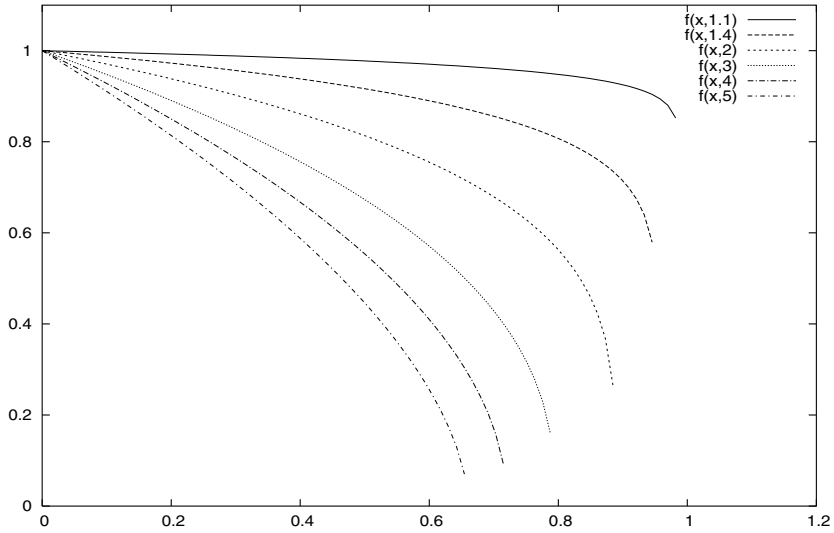

Figure 1. Illustration of the self-similar form of the cluster size distribution $f(\eta)$ for $w = 1.1$, 1.4, 2, 3, 4, 5, with $\alpha = 1, a = 1, b = 1$.

2.2. Accelerating input, $w > 1$

For large w, it may be assumed that monomers are added to the system so fast that the monomer concentration rises without limit. In this case we assume that $c_1 \sim Ct^\gamma$ with $\gamma > 0$, and $c_r(t) = c_1(t)\psi(r,t)$. Equation (1.3) then implies

$$\frac{1}{b}\frac{\partial\psi}{\partial t} + \frac{\gamma\psi}{bt} = \left(1 - \frac{aCt^\gamma}{b}\right)\frac{\partial\psi}{\partial r} + \frac{1}{2}\left(1 + \frac{aCt^\gamma}{b}\right)\frac{\partial^2\psi}{\partial r^2}. \tag{2.4}$$

From this we can see that the leading-order balance depends on the sign of γ. For $\gamma > 0$, if we assume that ψ varies slowly with r, then we have at leading order

$$\frac{1}{b}\frac{\partial\psi}{\partial t} + \frac{\gamma\psi}{bt} = -\frac{aCt^\gamma}{b}\frac{\partial\psi}{\partial r}. \tag{2.5}$$

This equation is solved by the similarity solution $\psi(r,t) = f(\eta)$ where $\eta = r/t^{1+\gamma}$,

$$f(\eta) = \begin{cases} \left(1 - \dfrac{(\gamma+1)\eta}{aC}\right)^{\gamma/(\gamma+1)} & \eta < \eta_c := \dfrac{aC}{\gamma+1} \\ 0 & \eta > \eta_c \end{cases} \tag{2.6}$$

and the constant of integration has been determined from the boundary condition $f(0) = 1$. However, C and γ remain to be determined. The shape of $f(\eta)$ is illustrated in figure 1, for a range of w-values.

To find C and γ we carry out a similar analysis to that above, but on equation (1.2), which yields

$$\frac{\gamma}{bt} = \frac{\alpha t^{w-\gamma}}{bC} - 1 - \left(\frac{aCt^\gamma}{b} - 1\right)\int_{\eta=0}^{\infty} f(\eta)\,\mathrm{d}\eta\, t^{1+\gamma}, \tag{2.7}$$

where $\eta(r,t) = r/t^{1+\gamma}$ describes the similarity solution for $\psi(r,t)$. At leading order, the balance is between the input term involving which is $\mathcal{O}(t^{w-\gamma})$ and the loss term which is $\mathcal{O}(t^{1+2\gamma})$. This implies that

$$\gamma = \tfrac{1}{3}(w-1), \qquad \text{and} \qquad C = ((1+2w)\alpha/3a^2)^{1/3}; \tag{2.8}$$

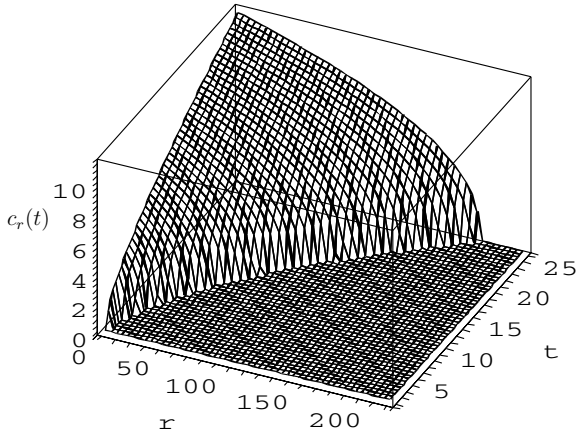

Figure 2. Illustration of the self-similar form of the cluster size distribution $c_r(t)$ with $w = 3, \alpha = 1, a = 1, b = 1$.

thus

$$c_1(t) \sim \left(\frac{(1+2w)\alpha}{3a^2}\right)^{1/3} t^{(w-1)/3}, \qquad c_r(t) \sim c_1(t)\, f(r/t^{(w+2)/3}), \tag{2.9}$$

where $f(\eta)$ is given by (2.6). Since this solution is only valid for $\gamma > 0$, it corresponds to the case $w > 1$.

The evolution of a cluster of large size $r \gg 1$ follows a two-stage process: firstly, the concentration remains small for a long time. Since the front moves so that its position is given by $r = (9\alpha a(1+2w))^{1/3} t^{(w+2)/3}/(w+2)$, it takes a time $t_c(r) \sim ((w+2)^3 r^3/9\alpha a(1+2w))^{1/(w+2)}$ to reach the cluster size $r \gg 1$. After this, there is a rapid phase of growth during which the concentration rises to $\mathcal{O}(t^{(w-1)/3})$, and in the second phase the concentration c_r continues to grow, asymptoting to $c_1(t)$ given by (2.9). This behaviour can be seen in figure 2.

2.3. The case $w = 1$

The problem of input with $w = 1$ is related to a previously studied case, since it corresponds to the constant monomer form of the Becker–Döring equations. However, with input, the large-time limit of the monomer concentration is *a priori* unknown and depends on the input parameter α.

First we assume that $c_1 \to C$ as $t \to \infty$, and then write the other concentrations as $c_r = C\psi(r,t)$. For large r the quantity $\psi(r,t)$ is then determined by the continuum limit equation

$$\frac{\partial \psi}{\partial t} = \frac{1}{2}(aC+b)\frac{\partial^2 \psi}{\partial r^2} - (aC-b)\frac{\partial \psi}{\partial r}. \tag{2.10}$$

Imposing the boundary conditions $\psi = 1$ at $r = 1$ and $\psi \to 0$ as $r \to \infty$, we find the solution

$$\psi = \frac{1}{2}\,\mathrm{erfc}\left(\frac{r - s(t)}{\sqrt{2(aC+b)t}}\right) \tag{2.11}$$

with $s(t) = aC - b$. For this solution we have $M_1 \sim \frac{1}{2}s^2 C$, and so $\dot{M}_1 \sim C(aC-b)^2)t$ as $t \to \infty$; this solution corresponds to input of the form αt with

$$\alpha = C(aC-b)^2. \tag{2.12}$$

This equation determines the remaining unknown parameter C in terms of α.

For large α, C can be approximated by

$$C \sim (\alpha/a^2)^{1/3}, \qquad \text{so that} \quad s(t) \sim (\alpha a)^{1/3} t, \tag{2.13}$$

and we see that the input is so fast that the monomer concentration is determined by a balance of the input rate α and the aggregation rate a, that is the parameters which determine how fast the monomer is added and how fast it can be used up in aggregation processes. The fragmentation rate plays no role in determining C. For small α the appropriate approximation is

$$C \sim b/a + \sqrt{\alpha/ab}, \qquad \text{so that} \quad s(t) \sim \sqrt{\frac{\alpha a}{b}}\, t, \tag{2.14}$$

and we see that the monomer concentration is only slightly above the largest possible for an equilibrium solution to exist. In particular we see that at leading order the input rate plays no role at all, we simply have $C \sim b/a$, so that the monomer concentration is a balance of aggregation and fragmentation rates. Only in the first order correction term does the presence of the input term influence the monomer concentration.

2.4. The case $0 < w < 1$

As in the case $w = 1$ we now have $\gamma = 0$; and as suggested by the small α limit of the case $w = 1$, namely (2.14), we have $C = b/a$. Formally the leading order balance in (2.7) is then between the two terms in large brackets. However, to fully determine the leading order expressions for the concentrations $c_r(t)$, we need to know the first correction term to the monomer concentration, hence we postulate

$$c_1(t) \sim \frac{b}{a}(1 + Ct^{-p}), \qquad \text{as} \quad t \to \infty, \tag{2.15}$$

$$c_r(t) \sim \frac{b}{a}\psi(r, t). \tag{2.16}$$

From (1.3) we then obtain the partial differential equation

$$\frac{1}{b}\frac{\partial \psi}{\partial t} = \frac{\partial^2 \psi}{\partial r^2} - Ct^{-p}\frac{\partial \psi}{\partial r} \tag{2.17}$$

with leading order solution $\psi = H(s(t) - r)$, with the position of the wavefront, $s(t)$ given by $\dot{s} = bCt^{-p}$. We find a more accurate solution of (2.17) by transforming from r to $z = r - s(t)$, which yields $\psi_t = b\psi_{zz}$. These equations are solved by

$$s(t) \sim \frac{bCt^{1-p}}{1-p} \qquad \text{and} \qquad \psi = \frac{1}{2}\operatorname{erfc}\left(\frac{z}{2\sqrt{bt}}\right). \tag{2.18}$$

However, the quantities p and C remain undetermined; they are found from the equation for $\dot{c}_1$, namely (1.2). In place of (2.7) we have

$$-\frac{pbC_1 t^{-p-1}}{a} = \alpha t^w - \frac{b^2 C_1 t^{-p} s(t)}{a}. \tag{2.19}$$

At large-times, the two terms on the right-hand side form the leading order balance, implying $p = \frac{1}{2}(1 - w)$ and $C_1 = \sqrt{\alpha a(1 + w)/2b^3}$ (we take the positive root since we require $\dot{s} > 0$ in (2.18)). Thus we have

$$c_1(t) \sim \frac{b}{a} + \sqrt{\frac{\alpha(1+w)}{2abt^{1-w}}} \qquad \text{and} \qquad s(t) \sim \sqrt{\frac{2\alpha a t^{1+w}}{b(1+w)}}, \tag{2.20}$$

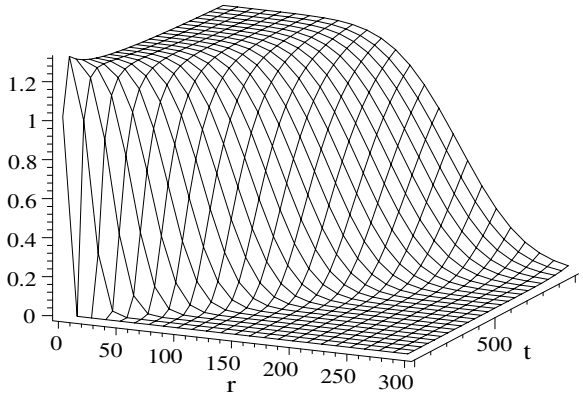

Figure 3. Illustration of the form of the cluster size distribution $c_r(t)$ at large-times, with $w = 0.5, \alpha = 1, a = 1, b = 1$.

wherein we note that the monomer concentration always approaches its equilibrium value from above, even though the initial data has $c_1(0) < b/a$. For small w in the range $0 < w < 1$, the monomer concentration approaches its equilibrium value with the difference decaying close to $1/\sqrt{t}$; however, for w near unity (and $w < 1$) the approach to equilibrium is extremely slow. The cluster size distribution is given by

$$c_r(t) \sim \frac{b}{2a} \operatorname{erfc}\left(\frac{r - s(t)}{2\sqrt{bt}}\right). \tag{2.21}$$

For w just below unity the diffusive wavefront moves to increasingly large aggregation numbers almost linearly in time ($r = s(t) = \mathcal{O}(t)$). For w just above zero, the diffusive wavefront moves to large aggregation numbers only slightly faster than $r = s(t) = \mathcal{O}(\sqrt{t})$. See figure 3 for an example where $w = 0.5$—the middle of the range $0 < w < 1$.

2.5. The case $w = 0$

As with the case $0 < w < 1$, the case $w = 0$ corresponds to keeping the monomer concentration fixed at $c_1 = b/a$; however, to determine the solution in the presence of continuous input, we again require knowledge of the first correction term to the monomer concentration in order to fully determine the solution for larger cluster sizes. The solution in this case is thus a generalization of the solution found in Wattis and King [25], since the extra parameter α, which determines the input rate, affects the solution. With $c_1 = b/a$, the aggregation and fragmentation effects are exactly balanced.

By continuity with the results of (2.20) in the limit $w \to 0$, we expect that at large times, the monomer concentration will be given by

$$c_1 = \left(\frac{b}{a}\right)\left(1 + \frac{\chi}{\sqrt{t}}\right). \tag{2.22}$$

The difference between the cases $w = 0$ and $w > 0$ occurs in the form of the size-distribution: when $w > 0$ 'advection' of matter to larger cluster sizes dominated diffusion as is seen through $s(t) \gg \sqrt{t}$ in (2.20). When $w = 0$ we expect the $s(t)/\sqrt{t}$ term in (2.21) to become a constant.

We follow the analysis of earlier sections, and write $c_r(t) = b\psi/a$ for large r and large t, obtaining

$$\frac{\partial \psi}{\partial t} = b\frac{\partial^2 \psi}{\partial r^2} - \frac{b\chi}{\sqrt{t}}\frac{\partial \psi}{\partial r}, \tag{2.23}$$

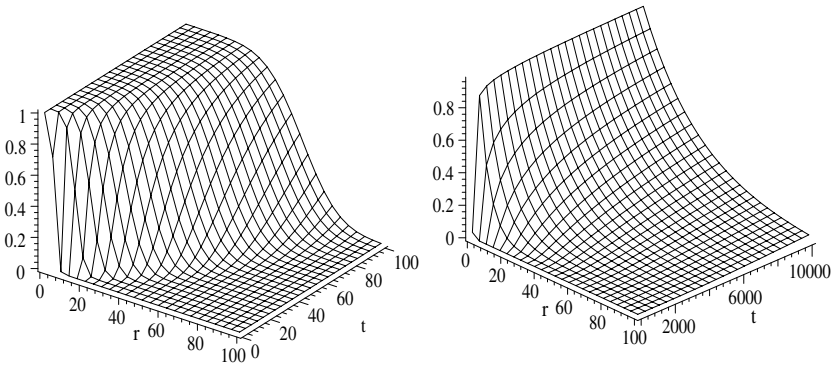

Figure 4. The similarity solution given by (2.24), in the case $b = 1$, $\chi = +3$ (left) and $\chi = -3$ (right).

which has a similarity solution of the form $\psi = \psi(r/\sqrt{t})$. Equation (2.23) is subject to the boundary conditions $\psi(r, t) \to 0$ as $r \to \infty$ and $\psi(1, t) = 1$. The solution of (2.23) is then

$$\psi = \frac{\operatorname{erfc}((r/2\sqrt{bt}) - \chi\sqrt{b})}{\operatorname{erfc}(-\chi\sqrt{b})}. \tag{2.24}$$

There remains the problem of determining the constant χ and how it depends on the input rate α.

We determine this by calculating the mass M_1 in two ways; from the input rate we have $M_1 \sim \alpha t$ as $t \to \infty$. Secondly, from the definition of the mass, $M_1 = \sum_{r=1}^{\infty} r c_r$, the formula $c_r(t) = (b/a)\psi(r, t)$ and the known form of ψ (2.24) we find

$$M_1 \sim \frac{4b^2 t}{a \operatorname{erfc}(-\chi\sqrt{b})} \int_0^{\infty} \eta \operatorname{erfc}(\eta - \chi\sqrt{b})\, \mathrm{d}\eta. \tag{2.25}$$

We thus have the equation

$$\frac{\alpha a}{4b^2} = 1 + 2\chi^2 b + \frac{2\chi\sqrt{b}\, \mathrm{e}^{-\chi^2 b}}{\sqrt{\pi} \operatorname{erfc}(-\chi\sqrt{b})} \tag{2.26}$$

for χ in terms of α. Whilst this is a transcendental equation for χ we can obtain the qualitative behaviour by considering it as an explicit equation for α in terms of χ, and evaluating the right-hand side in limits $\chi \to \pm\infty$.

Assuming a large positive value for χ we obtain the asymptotic formula $\chi \sim \sqrt{\alpha a/2b^3}$ valid for $\alpha \gg 1$. When $\chi = 0$ we have $\alpha = b^2/a$ and for χ large and negative, we obtain $\chi \sim -\sqrt{b/\alpha a}$ corresponding to $\alpha \to 0^+$ (using [1], equation 7.2.5). Thus as α ranges from small to large values, we obtain a variety of solutions, for which χ ranges from large negative to large positive values. The range of solutions is illustrated in figure 4.

The solution for $w = 0$ and large values of α (hence large positive χ) shares some common features with the solution for $w > 0$ in the limit $w \to 0$, notably the form of a moving diffusive wave. The solution we have generated, also includes the known solution for the constant monomer formulation of the Becker–Döring equations ($\chi = 0$ implies $\alpha = b^2/a$) and where the monomer concentration approaches its equilibrium value more quickly than the $t^{-1/2}$ convergence seen for other values of α. The result for small α (and hence large negative χ) may give us insight into the form of the solution in the region $w < 0$.

2.6. The case $-1 < w < 0$

In this case, even though the rate of input is decaying with time, the total mass in the system still diverges. Thus we expect the monomer concentration to again approach b/a but more slowly than in the above case. Including the correction term, the monomer concentration is now given by

$$c_1 \sim \frac{b}{a} - \frac{\chi}{t^{(w+1)/2}}, \tag{2.27}$$

which we see reduces to the above result in the case $w \to 0$ (2.22). The total number of clusters M_0 must then grow with $t^{(w+1)/2}$ in order to provide a leading order balance in the equation for M_0, namely

$$\dot{M}_0 = \alpha t^w + (b - ac_1)M_0 - bc_1. \tag{2.28}$$

The typical cluster size is then given by $M_1/M_0 \sim t^{(w+1)/2}$, and so we seek a similar solution in the variable $\eta = r/t^{(w+1)/2}$. We write the size-distribution function as $c_r = (b/a)\psi(r, t)$ and find

$$\frac{\partial \psi}{\partial t} = b\frac{\partial^2 \psi}{\partial r^2} + \frac{a\chi}{t^{(w+1)/2}}\frac{\partial \psi}{\partial r} \tag{2.29}$$

with the boundary conditions $\psi = 1$ at $r = 1$ and $\psi \to 0$ as $r \to \infty$. Assuming $\psi = f(\eta)$, we obtain $f'' + (a\chi/b)f' = 0$ with $f(0) = 1$ and $f(\eta) \to 0$ as $\eta \to \infty$ from which we deduce $f = \exp(-\chi a\eta/b)$.

It remains to determine χ, which is found, as in previous calculations, by evaluating the mass M_1. Given the above solution for ψ we obtain $M_1 \sim b^3 t^{w+1}/a^3\chi^2$ which, when set equal to $\alpha t^{w+1}/(w + 1)$, yields $\chi = (b/a)\sqrt{b(w + 1)/a\alpha}$.

In summary, as $t \to \infty$ we have

$$c_1 \sim \frac{b}{a}\left(1 - \sqrt{\frac{b(w + 1)}{a\alpha t^{w+1}}}\right), \qquad c_r \sim \frac{b}{a}\exp\left(-r\sqrt{\frac{b(w + 1)}{a\alpha t^{w+1}}}\right). \tag{2.30}$$

2.7. The case $w = -1$

This case is very similar to the case $-1 < w < 0$, with the complication that the scalings now involve terms in $\log t$, since the mass, M_1 scales according to $M_1 \sim \alpha \log t$. The characteristic size of clusters scales with $1/\sqrt{\log t}$. We have

$$c_1 \sim \frac{b}{a}\left(1 - \sqrt{\frac{b}{\alpha a \log t}}\right), \qquad c_r \sim \frac{b}{a}\exp\left(-r\sqrt{\frac{b}{\alpha a \log t}}\right) \tag{2.31}$$

as $t \to \infty$.

2.8. Summary

Table 1 summarizes the results for each of the cases detailed above. The leading order expressions for c_1, M_0 and $\langle r\rangle := M_1/M_0$ are all quoted. In all cases $M_1 = \alpha t^{w+1}/(w + 1)$. Note that the exponents of t are continuous across the special cases of $w = 1$ and $w = 0$ in the expressions for c_1, M_0 and $\langle r\rangle$.

For $w > 1$ the monomer concentration grows without bound (scaling with $t^{(w-1)/3}$), and the range of cluster sizes existent within the distribution scale with $t^{(w+2)/3}$. For $w \leqslant 1$ the monomer concentration saturates, and remains constant in the large time limit. For $w < 1$ the limiting concentration is the critical value of b/a. Note the difference in results between

Table 1. Summary of scaling behaviour for the Becker–Döring equations with fragmentation and aggregation. In all cases $M_1 = \sum_{r=1}^{\infty} r c_r = M_1(0) + \alpha t^{w+1}/(w+1)$; the average cluster size is given by $\langle r \rangle := M_1/M_0$.

w	c_1	M_0	$\langle r \rangle$
$w > 1$	$\left(\dfrac{(1+2w)\alpha t^{w-1}}{3a^2}\right)^{1/3}$	$\left(\dfrac{3\alpha^2 t^{1+2w}}{(1+2w)a}\right)^{1/3}$	$\left(\dfrac{\alpha a}{3}(1+2w)\right)^{1/3} \dfrac{t^{(w+2)/3}}{(1+w)}$
$w = 1$	$\underset{\alpha = C(aC-b)^2}{C > b/a}$	$(aC-b)Ct$	$\frac{\alpha t}{2(aC-b)C} = \frac{1}{2}(aC-b)t$
$0 < w < 1$	$\dfrac{b}{a} + \mathcal{O}(t^{(w-1)/2})$	$\sqrt{\dfrac{2\alpha b}{a(1+w)}}\, t^{(1+w)/2}$	$\sqrt{\dfrac{\alpha a}{2b(1+w)}}\, t^{(1+w)/2}$
$w = 0$	$\dfrac{b}{a} + \mathcal{O}(t^{-1/2})$	$\mathcal{O}(t^{1/2})$	$\mathcal{O}(t^{1/2})$
$-1 < w < 0$	$\dfrac{b}{a} + \mathcal{O}(t^{-(w+1)/2})$	$\sqrt{\dfrac{b\alpha t^{(w+1)}}{a(w+1)}}$	$\sqrt{\dfrac{a\alpha t^{(w+1)}}{b(w+1)}}$
$w = -1$	$\dfrac{b}{a}\left(1 - \sqrt{\dfrac{b}{\alpha a \log t}}\right)$	$\sqrt{\dfrac{b\alpha \log t}{a}}$	$\sqrt{\dfrac{a\alpha \log t}{b}}$

$0 < w < 1$ and $-1 < w < 0$; although the forms of M_0 and $\langle r \rangle$ are very similar, there are differences of a factor of $\sqrt{2}$ due to the 'advection' process which is present in the case of larger w, whereas for the smaller w the kinetics are due purely to diffusion in cluster size.

3. Irreversible aggregation

In the absence of aggregation, we can rescale time by the aggregation rate and so without loss of generality, it is sufficient to study the equations

$$\dot{c}_r = c_1(c_{r-1} - c_r) \tag{3.1}$$

$$\dot{c}_1 = \alpha t^w - c_1^2 - c_1 M_0 \tag{3.2}$$

$$\dot{M}_0 = \alpha t^w - c_1 M_0. \tag{3.3}$$

This corresponds to the system (1.2)–(1.3) with $b = 0$ and $a = 1$. We might expect such a simplification to the governing equations to make the ensuing analysis simpler, which it does, however, the end results for the behaviour of c_1 and the distribution c_r are no less complicated than the case for $b \neq 0$. Note that (3.2)–(3.3) form a closed system of two ordinary differential equations for (c_1, M_0), thus c_1 can be determined without knowing the full solution for $c_r(t)$ and $r > 1$.

3.1. General theory for the distribution of sizes

We assume that the concentrations follow a similarity solution of the form

$$c_r(t) \sim C t^{\gamma} f(\eta) \quad \text{with } f(0) = 1 \qquad \text{and} \qquad \eta = r/t^{\beta} \qquad \text{as } t \to \infty, \tag{3.4}$$

then $c_1 \sim C t^{\gamma}$. Thus we obtain qualitatively different behaviour for $\gamma > 0$, $\gamma = 0$ and $\gamma < 0$; the only restriction on parameters is $\beta > 0$.

The ordinary differential equation for $f(\eta)$ is obtained by an expansion of (3.1), which yields

$$\gamma C t^{\gamma-1} f(\eta) - \beta C t^{\gamma-1} \eta f'(\eta) = -C^2 t^{2\gamma-\beta} f'(\eta). \tag{3.5}$$

As $t \to \infty$ both terms on the lhs are of the same order of magnitude, so a balance of terms in this equation occurs when $\beta = 1 + \gamma$, then we have $\gamma f = (\beta\eta - C)f'$, which implies $f = K(C - \beta\eta)^{\beta/\gamma}$ for some constant K. The initial condition $f(0) = 1$ determines K, giving

$$f(\eta) = \begin{cases} (1 - (1+\gamma)\eta/C)^{\gamma/(1+\gamma)} & \eta < C/(1+\gamma) \\ 0 & \eta \geqslant C/(1+\gamma), \end{cases} \tag{3.6}$$

again we observe radically different qualitative behaviour for the cases $\gamma \lessgtr 0$. The condition $\beta > 0$ implies $\gamma > -1$.

To determine the remaining constants C and γ in terms of the given parameters α and w we turn to the equation for the total concentration M_0. Calculating the total number of clusters, M_0 from the above we find

$$M_0 \sim \sum_{r=1}^{Ct^\beta/\beta} c_r \sim \int_{\eta=0}^{C/\beta} Ct^\gamma \left(1 - \frac{(1+\gamma)\eta}{C}\right)^{\gamma/(1+\gamma)} t^\beta \, \mathrm{d}\eta \sim \frac{C^2 t^{1+2\gamma}}{1+2\gamma}. \tag{3.7}$$

The details as to which terms in (3.2) and (3.3) form the leading order balance, depend on the value of γ and hence on w. We thus consider each parameter range in turn.

3.2. Irreversible aggregation with $w > 1$

The case $w > 1$ arises from assuming $\gamma > 0$ in (3.4). As already noted (2.2), this arises from a balance in (3.3) and (3.2) of input (αt^w) and loss due to $M_0 c_1 \sim \mathcal{O}(t^{1+3\gamma})$. The leading order balance in both of these equations gives $\gamma = (w-1)/3$ and comparing coefficients of these terms we find $\alpha = C^3/(1+2\gamma)$, thus the monomer concentration is given by

$$c_1 \sim \left(\tfrac{1}{3}\alpha(1+2w)\right)^{1/3} t^{(w-1)/3} \qquad \text{as} \quad t \to \infty. \tag{3.8}$$

The distribution of sizes is given by $c_r(t) \sim c_1(t) f(r/t^{(w+2)/3})$ with the self-similar function $f(\eta)$ given by

$$f(\eta) = \begin{cases} \left(1 - \dfrac{w+2}{(9(1+2w))^{1/3}}\eta\right)^{\frac{(w-1)}{(w+2)}} & \eta < \eta_c := \dfrac{(9(1+2w))^{1/3}}{(2+w)} \\ 0 & \eta > \eta_c. \end{cases} \tag{3.9}$$

The maximum cluster size in the distribution is

$$r_m \sim \frac{(9(1+2w))^{1/3} t^{(w+2)/3}}{(w+2)}. \tag{3.10}$$

The behaviour described above is identical to the case of the Becker–Döring equations with fragmentation as studied in section 2.2, since as all concentrations grow arbitrarily large in time with the same exponent the aggregation terms, being the product of two concentrations form the leading order terms, the fragmentation terms are subdominant since they are proportional to a concentration.

3.3. Irreversible aggregation with $w = 1$

Taking the limit $w \to 1^+$ in the above section, we deduce that it is possible that c_1 approaches a constant as $t \to \infty$. Such a result will change the shape of the distribution, since the aggregation and fragmentation terms will then be of the same order of magnitude in the large-time limit. Much of the asymptotic structure for this case will be the same as that of the constant monomer concentration formulation of the Becker–Döring equations. The most important unresolved issue is to determine precisely to which constant the monomer concentration approaches.

The equation $\dot{M}_0 = \alpha t - c_1 M_0$ for M_0 implies

$$c_1 \sim C + \chi t^q, \qquad M_0 \sim \alpha t/C + m t^\mu, \tag{3.11}$$

for some constants C, m, χ, q, μ. A relationship between these can be established by solving the equations for M_0 and c_1 to second order. This yields $q = 1$, $\mu = 0$ and $m = -(\chi + 1)C$, leaving χ and more importantly C undetermined. These will be determined after the shape of the distribution has been found.

Writing $c_r(t) \sim C\psi(r, t)$, we have

$$\frac{1}{C}\frac{\partial \psi}{\partial t} = -\frac{\partial \psi}{\partial r} + \frac{1}{2}\frac{\partial^2 \psi}{\partial r^2}, \tag{3.12}$$

which at leading order is solved by $\psi = H(Ct - r)$. This is formally the solution given by (3.6) in the case $\gamma = 0$. To obtain the shape of the transition region near $r = Ct$, we put $r = Ct + z$, which yields $\psi_t = \frac{1}{2}C\psi_{zz}$, leading to the solution

$$\psi = \frac{1}{2}\operatorname{erfc}\left(\frac{r - Ct}{\sqrt{2Ct}}\right). \tag{3.13}$$

To determine C we calculate the mass in two ways. The quantity M_1 is given by $\dot{M}_1 = \alpha t$ so $M_1 = \frac{1}{2}\alpha t^2 + M_1(0)$. Also

$$M_1 = \sum_{r=1}^{\infty} r c_r \sim \sum_{r=1}^{Ct} rC \sim \frac{1}{2}C^3 t^2. \tag{3.14}$$

Thus $C = \alpha^{1/3}$, and although the form of ψ is no longer as simple as (3.9), formula (3.8) for C in terms of α and w remains valid. In summary we have

$$c_1 \sim \alpha^{1/3} + \mathcal{O}(t^{-1}), \qquad c_r \sim \frac{1}{2}\alpha^{1/3}\operatorname{erfc}\left(\frac{r - \alpha^{1/3}t}{\sqrt{2\alpha^{1/3}t}}\right) \qquad \text{as} \quad t \to \infty. \tag{3.15}$$

Note that this has the same form as the constant monomer case, and is similar to the form of the solution for the case with fragmentation, namely (2.11) with (2.12). In the presence of fragmentation, the monomer concentration has a limiting value which is dependent on the aggregation and fragmentation rates, but agrees with the above result in the limit of large α.

3.4. Irreversible aggregation with $-\frac{1}{2} < w < 1$

All the scalings as derived in section 3.1 remain valid in this case, however, note that there are qualitative differences in behaviour between this and the case $w > 1$. Firstly, since this case corresponds to $\gamma < 0$ the monomer concentration decays to zero instead of growing without bound, although the total number of clusters M_0 given by (3.7) diverges as $t \to \infty$. Secondly, the function $f(\eta)$ takes a qualitatively different form, now diverging at $\eta = \eta_c$ rather than taking the value zero and being continuous. An illustration of $f(\eta)$ for a range of values of w is given in figure 5.

The leading order balance in (3.3) remains that between the two terms on the right-hand side, so γ and C are given by the same formulae as in the case $w > 1$ (section 3.2). Hence (3.8) and (3.10) remain valid along with $c_r \sim c_1(t) f(r/t^{(w+2)/3})$ with $f(\eta)$ given by (3.9).

This case contains the special case $w = 0$ which can be analysed more simply by a variety of techniques, since equations (3.2) and (3.3) are then autonomous. This system has been rigorously analysed by centre-manifold theory and Poincaré compactification by da Costa *et al* [8], proving the validity of the above results. In section 3.8, we show that the distribution is not discontinuous across $r = r_m$, rather there is a boundary layer in which different scalings apply and provide a smooth transition across this region of rapid change.

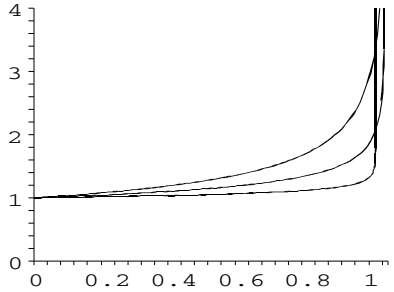

Figure 5. Illustration of the form of the self-similar cluster size distribution of the pure aggregation Becker–Döring system. The function $f(\eta)$ given by (3.9) is plotted against η for $w = 0.2$ (steepest curve), 0.5 (middle curve), and 0.8 (almost flat at $f = 1$ for $0 < \eta < 1$). Each value of w gives a different η_c where the curve diverges; for $\eta > \eta_c$, the distribution is given by $f = 0$.

3.5. Irreversible aggregation with $w = -\frac{1}{2}$

This is a special borderline case, which qualitatively has the same behaviour as $-\frac{1}{2} < w < 1$, but the details of the scalings include log terms. In particular, we consider the equation $\widetilde{M}_0 = c_1^2$ where $\widetilde{M}_0 = M_0 - c_1$ and (3.2), and to satisfy the leading order balance in these equations we require

$$\begin{aligned} &c_1 \sim \left(\tfrac{1}{3}\alpha\right)^{1/3} t^{-1/2} (\log t)^{-1/3}, \\ &M_0 \sim \widetilde{M}_0 \sim (3\alpha^2)^{1/3} (\log t)^{1/3} \qquad \text{as} \quad t \to \infty. \end{aligned} \tag{3.16}$$

We then find the size-dependence of the distribution scales according to similarity variable $\eta = r(\log t)^{1/3}/t^{1/2}$, yielding an equation for $f(\eta)$ of the form

$$-\tfrac{1}{2} f - \tfrac{1}{2}\eta f' = -\left(\tfrac{1}{3}\alpha\right)^{1/3} f', \tag{3.17}$$

which is solved by $f(\eta) = 1\big/\left(1 - \frac{1}{2}\left(\frac{1}{3}\alpha\right)^{-1/3}\eta\right)$, which, however, is not integrable. The cluster of maximum size thus scales with time according to $r_m \sim 2\left(\frac{1}{3}\alpha\right)^{1/3} t^{1/2} (\log t)^{-1/3}$.

3.6. Irreversible aggregation with $-1 \leqslant w < -\frac{1}{2}$

In this case the total number of clusters M_0 saturates, that is tends to a nonzero constant in the large time limit, whilst the monomer concentration decays. This is most easily seen if we consider the equation $\widetilde{M}_0 = c_1^2$ for $\widetilde{M}_0 = M_0 - c_1 = \sum_{r=2}^{\infty} c_r$.

We thus find the large-time asymptotic behaviour for M_0, c_1 is as follows:

$$M_0 \sim \widetilde{M}_0 \sim K, \qquad c_1 \sim \frac{\alpha}{K} t^w \qquad \text{as} \quad t \to \infty \tag{3.18}$$

for some constant K which depends on the initial data. Note that with $\gamma = w$, the function $f(\eta)$ is not integrable, thus there is no self-similar size distribution in this case. The interpretation of this is that the kinetics are so slow that the system always retains a memory of its initial data.

3.7. Summary

See table 2 for a summary of the large time behaviours of c_1, M_0 and the ratio M_1/M_0 which gives the average cluster size in the system. For $w < -1$ the mass of the system and the kinetics depends at leading order on the initial conditions, and therefore typically there is no self-similar behaviour observed.

Table 2. Summary of scaling behaviour for pure aggregation equations. In all cases $M_1 = \sum_{r=1}^{\infty} r c_r = M_1(0) + \alpha t^{w+1}/(w+1)$; the average cluster size is given by $\langle r\rangle := M_1/M_0$. For $w \leqslant -\frac{1}{2}$ there are no similarity solutions.

w	c_1	M_0	$\langle r\rangle$
$w > 1$	$\left(\frac{1}{3}\alpha(1+2w)\right)^{1/3} t^{(w-1)/3}$	$\left(\frac{3\alpha}{1+2w}\right)^{1/3} t^{(1+2w)/3}$	$\frac{(\alpha(1+2w))^{1/3}}{3^{1/3}(1+w)} t^{(2+w)/3}$
$w = 1$	$\alpha^{1/3} + \mathcal{O}(t^{-1})$	$\alpha^{2/3} t$	$\frac{1}{2}\alpha^{1/3} t$
$-\frac{1}{2} < w < 1$	$\left(\frac{1}{3}\alpha(1+2w)\right)^{1/3} t^{(w-1)/3}$	$\left(\frac{3\alpha}{1+2w}\right)^{1/3} t^{(1+2w)/3}$	$\frac{(\alpha(1+2w))^{1/3}}{3^{1/3}(1+w)} t^{(2+w)/3}$
$w = -\frac{1}{2}$	$\left(\frac{1}{3}\alpha\right)^{1/3} t^{-1/2} (\log t)^{-1/3}$	$(3\alpha^2)^{1/3} (\log t)^{1/3}$	$\left(\frac{8}{3}\alpha\right)^{1/3} t^{1/2} (\log t)^{-1/3}$
$-1 \leqslant w < -\frac{1}{2}$	$\frac{\alpha t^w}{C_0}$	C_0	$\mathcal{O}(t^{w+1})$

3.8. Higher order analysis for $-\frac{1}{2} < w < 1$

Once the large-time behaviour of c_1 and M_0 has been determined, there is an alternative way of deriving the size-dependence of the distribution which we shall now describe. The advantage of the formulation presented below is that it enables higher-order effects to be determined, and we shall show how the discontinuity at $r = r_m$ given by (3.10) is smoothed.

In the large-time limit, the c_r variables are found by making the substitution $c_r(t) = c_1(t)\psi(r,t)$, where r is treated as a continuous variable. With τ defined such that $\mathrm{d}/\mathrm{d}\tau = (1/c_1)\,\mathrm{d}/\mathrm{d}t$ we obtain

$$\frac{\partial\psi}{\partial\tau} = -\frac{\psi}{c_1}\frac{\mathrm{d}c_1}{\mathrm{d}\tau} - \frac{\partial\psi}{\partial r} + \frac{1}{2}\frac{\partial^2\psi}{\partial r^2}. \tag{3.19}$$

From section 3.4 we know that $c_1 \sim \mathcal{O}(t^{(w-1)/3})$ thus $\tau \sim \mathcal{O}(t^{(w+2)/3})$ and $c_1(\tau) = \mathcal{O}(\tau^{\nu})$ where $\nu = -(w-1)/(w+2)$. As w ranges from $-\frac{1}{2}$ to unity, the parameter ν varies from -1 to zero.

At leading order, the second derivative term in (3.19) may be ignored, leaving an equation which has the similarity solution $\psi(r,t) = f(\widehat{\eta})$ with $\widehat{\eta} = r/\tau$ with $f(0) = 1$ and $f(\infty) = 0$ (note that $\widehat{\eta}$ differs from η in sections 3.2 and 3.4 only through a rescaling by a constant, so that the discontinuity is at $\widehat{\eta} = 1$). The function $f(\widehat{\eta})$ satisfies $(1-\widehat{\eta})f' = \nu f$ where ν is the exponent of the decay of $c_1(\tau)$; thus f is given by

$$f(\widehat{\eta}) = \begin{cases} \dfrac{1}{(1-\widehat{\eta})^{\nu}} & \widehat{\eta} < 1 \\ 0 & \widehat{\eta} \geqslant 1. \end{cases} \tag{3.20}$$

Note that this is the same result as (3.9).

The discontinuity at $\widehat{\eta} = 1$ can be smoothed by considering the second order derivative in (3.19). We transform from r to $z = r - \tau$ with $z \ll \tau$ and hence obtain

$$\frac{\partial\psi}{\partial\tau} = \frac{1}{2}\frac{\partial^2\psi}{\partial z^2} + \frac{\nu\psi}{\tau}. \tag{3.21}$$

This equation possesses self-similarity solutions of the form $\psi = h(\tau)g(\xi)$ with $\xi = z/\sqrt{\tau}$. For $z \ll -1$ we require the solution of this PDE to match with the solution $\psi = f$ given by (3.20). Such a match implies $\psi \sim \tau^{\nu/2}(-\xi)^{-\nu}$ as $\xi \to -\infty$ hence $h(\tau) = \tau^{\nu/2}$. Equation (3.21) then becomes

$$g'' + \xi g' + \nu g = 0, \tag{3.22}$$

which has the solutions

$$g_1(\xi) = \frac{\mathrm{e}^{-\xi^2/4}}{\sqrt{\xi}} M_{-\frac{1}{4}+\frac{1}{2}\nu,\frac{1}{4}}\left(\frac{1}{2}\xi^2\right), \qquad g_2(\xi) = \frac{\mathrm{e}^{-\xi^2/4}}{\sqrt{\xi}} W_{-\frac{1}{4}+\frac{1}{2}\nu,\frac{1}{4}}\left(\frac{1}{2}\xi^2\right), \tag{3.23}$$

where $M_{\kappa,\mu}(z)$ and $W_{\kappa,\mu}(z)$ are Whittaker's functions [1]. The functions g_1, g_2 are real-valued in $\xi > 0$, but pure imaginary in $\xi < 0$, satisfying $\mathrm{i}g_1(\xi) = g_1(-\xi)$ and $\mathrm{i}g_2(\xi) = g_2(-\xi)$ for $\xi < 0$.

Solutions to the differential equation valid on $\xi \in \mathbb{R}$ can be constructed by piecing together g_1 and g_2 with real and imaginary premultiplicative constants, or by constructing even and odd functions according to

$$g_3(\xi) = H(\xi)g_1(\xi) - H(-\xi)g_1(-\xi) = \frac{\xi\,\mathrm{e}^{-\xi^2/2}}{2^{3/4}} M\left(1-\frac{1}{2}\nu, \frac{3}{2}; \frac{1}{2}\xi^2\right) \tag{3.24}$$

$$g_4(\xi) = H(\xi)g_2(\xi) + H(-\xi)g_2(-\xi) = \frac{|\xi|\,\mathrm{e}^{-\xi^2/2}}{2^{3/4}} U\left(1-\frac{1}{2}\nu, \frac{3}{2}; \frac{1}{2}\xi^2\right) \tag{3.25}$$

$$g_5(\xi) = H(\xi)g_1(\xi) + H(-\xi)g_1(-\xi) = \frac{|\xi|\,\mathrm{e}^{-\xi^2/2}}{2^{3/4}} M\left(1-\frac{1}{2}\nu, \frac{3}{2}; \frac{1}{2}\xi^2\right), \tag{3.26}$$

where $H(\cdot)$ is the Heaviside function and $M(\cdot,\cdot;\cdot)$ and $U(\cdot,\cdot;\cdot)$ are Kummer's hypergeometric functions [1]. Here, g_3 is smooth odd and positive in $\xi > 0$ whilst both g_4 and g_5 are even and positive for all ξ; however, g_4 and g_5 suffer from a discontinuous first derivative at $\xi = 0$. By forming a linear combination of g_4 and g_5, we construct the smooth even function

$$g_6(\xi) = 2^{3/4}g_5(\xi) + \frac{\Gamma\left(\frac{1}{2}-\frac{1}{2}\nu\right)}{2^{1/4}\sqrt{\pi}} g_4(\xi). \tag{3.27}$$

which is positive for all ξ and solves the differential equation (3.22).

Now to satisfy the boundary condition $g \to 0$ as $\xi \to \infty$ we take a linear combination of g_3 and g_6 which has the most rapid decay at large ξ. Since $g_3 \sim 2^{\nu/2-5/4}\sqrt{\pi}\xi^{-\nu}/\Gamma\left(1-\frac{1}{2}\nu\right)$ and $g_6 \sim 2^{\nu/2-1/2}\sqrt{\pi}\xi^{-\nu}/\Gamma\left(1-\frac{1}{2}\nu\right)$ as $\xi \to \infty$, this leads to the solution

$$g(\xi) = K(g_6(\xi) - 2^{3/4}g_3(\xi)), \tag{3.28}$$

for some constant $K > 0$. The function g is positive for all ξ, has a maximum in $\xi < 0$ and decays monotonically to zero as $\xi \to \infty$. The premultiplicative constant K is chosen to ensure that $g(\xi) \sim (-\xi)^{-\nu}$ as $\xi \to -\infty$ in order that $g(\xi)$ matches correctly back into $f(\widehat{\eta})$ as $\widehat{\eta} \to 1^-$. This condition gives $K = \Gamma\left(1-\frac{1}{2}\nu\right)/2^{\nu/2+1/2}\sqrt{\pi}$. Writing g in terms of Kummer's hypergeometric functions we have

$$g(\xi) = \frac{\Gamma\left(1-\frac{1}{2}\nu\right)|\xi|\,\mathrm{e}^{-\xi^2/2}}{2^{\nu/2-1/2}\sqrt{\pi}} \left(\frac{\Gamma\left(\frac{1}{2}-\frac{1}{2}\nu\right)}{4\sqrt{\pi}} U\left(1-\frac{1}{2}\nu, \frac{3}{2}; \frac{1}{2}\xi^2\right) + H(-x)M\left(1-\frac{1}{2}\nu, \frac{3}{2}; \frac{1}{2}\xi^2\right)\right). \tag{3.29}$$

This is plotted in figure 6. We observe a well defined peak when ν is near unity, corresponding to $w = -\frac{1}{2}$; and the peak diverges as $\nu \to 1$, coinciding with the point $w = -\frac{1}{2}$, where $f(\eta)$ ceases to be integrable. For w near unity, which corresponds to ν near zero, the peak is not well defined, and appears more like a smooth transition from one plateau at $g \approx 1$ to another plateau at $g = 0$. Thus we observe a qualitative matching into the behaviour of the special case $w = 1$ which has the form of a diffusive wave with erfc shape joining the steady states $c_r = c_1$ and $c_r = 0$.

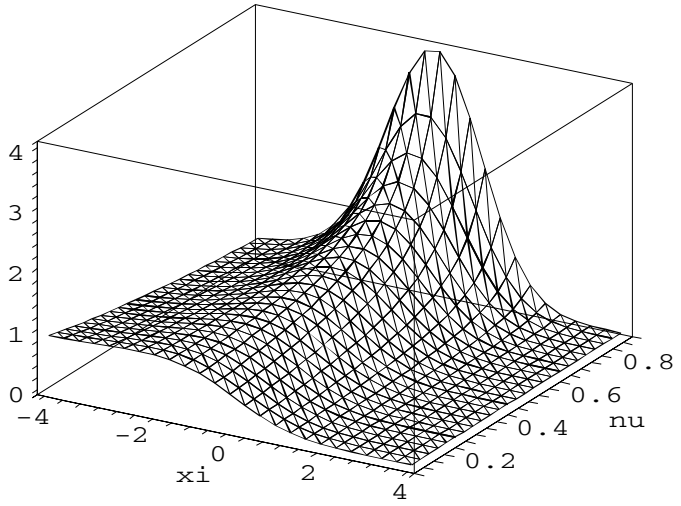

Figure 6. Illustration of the form of the spike in the distribution of the pure aggregation Becker–Döring system. The function $g(\xi)$ given by (3.29) is plotted against ξ for $0.1 < \nu < 0.9$.

From the scalings introduced at the start of this section, note that the amplitude of the spike decays with $\mathcal{O}(t^{(w-1)/6})$ which is half of the exponent of $c_1(t) = \mathcal{O}(t^{(w-1)/3})$. The width of the spike is given by $\xi = \mathcal{O}(1)$ so in terms of the aggregation number, r, the width of the peak scales with $\mathcal{O}(t^{(w+2)/6})$.

4. Discussion

In this paper we have analysed the Becker–Döring equations with a range of time-dependent monomer input functions of the form αt^w. Since the monomer concentration is unknown and has to be solved for as part of the problem, this formulation of the problem is more complex than the often-studied constant monomer formulation of the Becker–Döring equations, or the constant mass formulation. The system forms a useful contribution to the study of more complex physicochemical processes in which a precursor species decays to provide the monomeric material from which clusters grow, such as micelle- or vesicle-formation [9, 10].

We have found a variety of self-similar behaviours in the case where aggregation and fragmentation rates are size-independent. We have considered the aggregation-fragmentation form of the Becker–Döring equations as well as the pure aggregation formulation. In both formulations when the monomer input exponent satisfies $w > 1$, there are similarity solutions in which the monomer concentration has the largest concentration of any cluster size present in the system. While the solution approaches the steady-state solution $c_r(t) = c_1(t)$; at all times there is a maximum cluster size beyond which virtually no clusters have yet formed. This maximum cluster size grows with $t^{(w+2)/3}$; this behaviour is seen in both the systems with and without fragmentation.

For the cases $0 < w < 1$, in the presence of fragmentation, the cluster-size distribution takes on the form of a diffusive wave which propagates through the space of cluster sizes to increasingly large sizes, while broadening out. The front moves so that almost all clusters in the system have a size $r < s(t)$ with $s(t)$ given by (2.20). Clusters behind the front, have concentrations which approach the critical concentration b/a. For the power w in the range $-1 < w < 0$, the concentrations approach b/a by a purely diffusive process.

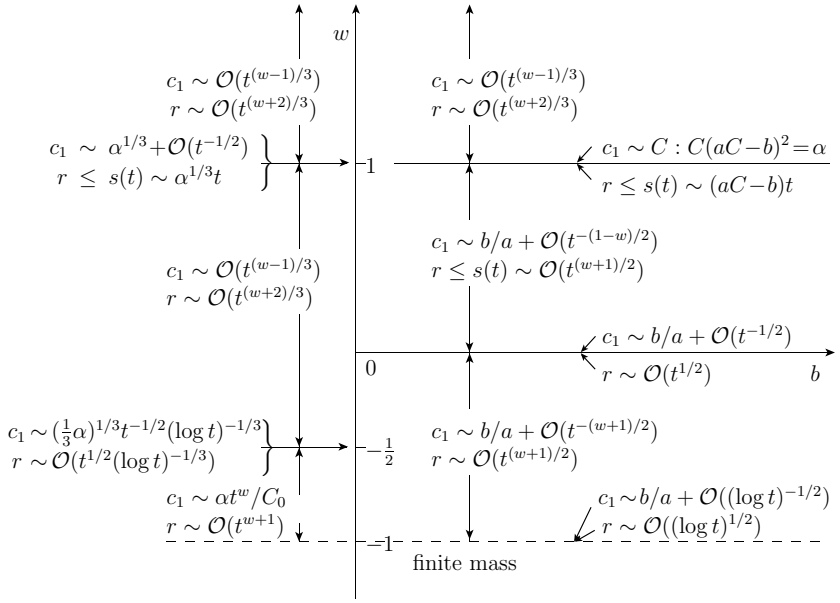

Figure 7. Summary of parameter regimes, and the scalings valid within each.

For the case $w < -1$, the total mass of the system approaches a finite constant value, and so the large-time asymptotics are dominated by the convergence to an equilibrium solution of the correct value for the total mass in the system. This scenario is not nearly so interesting as the two regimes described above, and so has been omitted for the sake of space. In the special cases $w = 1, 0, -1$, 'crossover' behaviour is observed; these cases exhibiting some features of each of their neighbouring generic cases.

In the absence of fragmentation, the only active process is aggregation and only in the case of $w = 1$ do concentrations approach a nonzero constant. This case has dynamics similar to those observed in systems with fragmentation. When $w > 1$ all concentrations grow without bound, as noted above; when $w < 1$, all concentrations approach zero in the large-time limit. This occurs by a distribution which has a large spike near the maximum cluster size in the system. Whilst decaying in amplitude, this spike moves to increasingly large cluster sizes, leaving the concentrations behind to decay back to zero at an algebraic rate.

For a rigorous analysis of the problem of monomer input into an aggregating system without fragmentation in the case $w = 0$, see the paper by da Costa *et al* [8]. In this case, the concentrations behind the spike decay as $t^{-1/3}$, whereas the spike moves to larger sizes so that its position is at $r = \mathcal{O}(t^{2/3})$ in a way such that the concentration of cluster sizes in the spike decays as $t^{-1/6}$. Here, we have given a more complete description of the problem of monomer input into a system with no fragmentation. Whilst the analysis of section 3.8 is not as rigorous as that presented in [8], the analysis of the wide range of parameter space $w > -1$ provides a more complete picture of the behaviour of such systems. A full summary of the scaling exponents for the monomer concentration and the typical cluster size for systems with fragmentation and without is given in figure 7.

The cluster distribution functions of section 3 show similar qualitative features to the results of the 'γ-hook' models analysed by Brilliantov and Krapivsky [5], that is, a distribution which has a maximum cluster size, a peak in the distribution close to the maximum cluster size, and a plateau of lower concentrations at smaller cluster sizes ranging back to the monomer.

These 'hook' models correspond to the Becker–Döring system with constant input ($w = 0$ in our terminology) and rate coefficients of the form $a_r = ar^\gamma$ (rather than our assumption of $a_r = a$).

Whilst the models of epitaxial growth used by Gibou *et al* [13] are not identical to ours (due to their use of size-dependent growth rates), we note that it has the form of a pure aggregation Becker–Döring system; figures 3 and 4 of their work show a striking similarity with figure 6 of this paper. Similar comments hold for the results presented by Evans and Bartelt [12] (figures 2 and 8) and, to a lesser extent, to Bales and Chrzan [2].

It is hoped that the methods described above will be of use in more general problems, for example those which involve size-dependent aggregation and fragmentation rates, and systems in which the time-dependent monomer release is given by more complex functions, for example, the cases of micelle- and vesicle-formation which have been studied previously [9, 10].

Acknowledgments

I would like to thank Colin Bolton, who performed preliminary numerical calculations which initiated this work. I am grateful to Fernando da Costa for many interesting discussions on the systems analysed here. My thanks also go to the British Council, Portugal and CRUP for funding visits to Lisbon, where some of this work was carried out. My thanks also go to Bob Pego and Barbara Niethammer for inviting me to a SIAM meeting where I discovered the links between this work and models of epitaxial growth.

References

[1] Abramowitz M and Stegun I A 1972 *Handbook of Mathematical Functions* (New York: Dover)
[2] Bales G S and Chrzan D C 1994 Dynamics of irreversible island growth during submonolayer epitaxy *Phys. Rev.* B **50** 6057–67
[3] Becker R and Döring W 1935 Kinetische behandlung der Keimbildung in ubersattigten dampfern *Ann. Phys.* **24** 719–52
[4] Blackman J A and Marshall A 1994 Coagulation and fragmentation in cluster-monomer reaction models *J. Phys. A: Math. Gen.* **27** 725–40
[5] Brilliantov N V and Krapivsky P 1991 Nonscaling and source-induced scaling behaviour in aggregation models of movable monomers and immovable clusters *J. Phys. A: Math. Gen.* **24** 4787–803
[6] Bolton C D and Wattis J A D 2004 The Becker–Döring equations with constant monomer input, competition and inhibition *J. Phys. A: Math. Gen.* **37** 1971–86
[7] da Costa F P 1996 On the dynamic scaling behaviour of solutions to the discrete Smoluchowski equation *Proc. Ed. Math. Soc.* **39** 547–59
[8] da Costa F P, van Roessel H and Wattis J A D 2004 Long-time behaviour and self-similarity in a coagulation equation with input of monomers *Preprint* nlin.AO/0402037
[9] Coveney P V and Wattis J A D 1996 Analysis of a generalized Becker–Doring model of self-reproducing micelles *Proc. R. Soc.* A **452** 2079–102
[10] Coveney P V and Wattis J A D 1998 A Becker-Doring model of self-reproducing vesicles *J. Chem. Soc. Faraday Trans.* **102** 233–46
[11] Davies S C, King J R and Wattis J A D 1999 The Smoluchowski coagulation equations with continuous injection *J. Phys. A: Math. Gen.* **32** 7745–63
[12] Evans J W and Bartelt M C 1996 Nucleation, growth and kinetic roughening of metal (100) homoepitaxial thin films *Langmuir* **12** 217–29
[13] Gibou F, Ratsch C and Caflisch R 2003 Capture numbers in rate equations and scaling laws for epitaxial growth *Phys. Rev.* B **67** 155403
[14] King J R and Wattis J A D 2002 Asymptotic solutions of the Becker–Doring equations with size-dependent rate constants *J. Phys. A: Math. Gen.* **35** 1357–80

[15] Krapivsky P and Redner S 1996 Transitional aggregation kinetics in dry and damp environments *Phys. Rev.* E **54** 3553–61
[16] Kreer M and Penrose O 1994 Proof of dynamic scaling in Smoluchowski's coagulation equations with constant kernels *J. Stat. Phys.* **74** 389–407
[17] Leyvraz F 2003 Scaling theory and exactly solved models in the kinetics of irreversible aggregation *Phys. Rep.* **383** 95–212
[18] Leyvraz F and Tschudi H R 1981 Singularities in the kinetics of coagulation processes *J. Phys. A: Math. Gen.* **14** 3389–405
[19] Lushnikov A A and Kulmala M 2001 Nonsingular self-preserving regimes of coagulation-condensation process *Phys. Rev.* E **64** 031605
[20] Lushnikov AA and Kulmala M 2002 Singular self-preserving regimes of coagulation processes *Phys. Rev.* E **65** 041604
[21] Menon G and Pego R L 2003 Approach to self-similarity in Smoluchowski's coagulation equations *Preprint* nlin.AO/0306047
[22] Menon G and Pego R L 2003 Dynamical scaling in Smoluchowski's coagulation equations: uniform convergence *Preprint* nlin.AO/0306048
[23] Penrose O and Lebowitz J 1976 *Studies in Statistical Mechanics VII: Fluctuation Phenomena* ed E Montroll and J L Lebowitz (Amsterdam: North-Holland) pp 322–75
[24] von Smoluchowski M 1916 Drei vorträge über diffusion, brownsche molekular bewegung und koagulation von kolloidteichen *Physik. Z.* **17** 557
[25] Wattis J A D and King J R 1998 Asymptotic solutions of the Becker-Doring equations *J. Phys. A: Math. Gen.* **31** 7169–89